Inorganic Chemistry
Article

*Inorg. Chem.* **2010**, *49*, 10007–10012 **10007**
DOI: 10.1021/ic1013285

# Importance of Energy Level Matching for Bonding in $Th^{3+}$-$Am^{3+}$ Actinide Metallocene Amidinates, $(C_5Me_5)_2[^iPrNC(Me)N^iPr]An$

**Justin R. Walensky,[†,‡] Richard L. Martin,[*,‡] Joseph W. Ziller,[†] and William J. Evans[*,†]**

[†]*Department of Chemistry, University of California, Irvine, California 92697-2025, United States, and* [‡]*Theoretical Division, Los Alamos National Laboratory, MS-B268, Los Alamos, New Mexico 87545, United States*

Received July 2, 2010

The synthesis of a rare trivalent $Th^{3+}$ complex, $(C_5Me_5)_2[^iPrNC(Me)N^iPr]Th$, initiated a density functional theory analysis on the electronic and molecular structures of trivalent actinide complexes of this type for An = Th, Pa, U, Np, Pu, and Am. While the 6d orbital is found to accommodate the unpaired spin in the $Th^{3+}$ species, the next member of the series, Pa, is characterized by an $f^2$ ground state, and later actinides successively fill the 5f shell. In this report, we principally examine the evolution of the bonding as one advances along the actinide row. We find that the early actinides (Pa−Np) are characterized by localized f orbitals and essentially ionic bonding, whereas the f orbitals in the later members of the series (Pu, Am) exhibit significant interaction and spin delocalization into the carbon- and nitrogen-based ligand orbitals. This is perhaps counter-intuitive since the f orbital radius and hence metal−ligand overlap decreases with increasing Z, but this trend is counter-acted by the fact that the actinide contraction also leads to a stabilization of the f orbital manifold that leads to a near degeneracy between the An 5f and cyclopentadienyl $\pi$-orbitals for Pu and Am, causing a significant orbital interaction.

## Introduction

A long-standing debate in actinide chemistry centers on the role that 5f orbitals play in actinide-ligand bonding. The generally accepted understanding is that early members of the actinide series may exhibit significant metal−ligand mixing (bonding), but that the interaction is largely mediated by the actinide 6d orbitals with the actinide 5f manifold being essentially uninvolved.[1] The reason for this behavior lies in the small 5f orbital radius compared with that of the 6d, which results in limited overlap between 5f and ligand orbitals. This picture, taken to its extreme, suggests that the actinide 5f manifold is largely a reservoir for the additional charge as *Z* increases across the row.

This is not to say, however, that there is no involvement of the 5f orbitals in organoactinide chemistry. Several examples are in the literature where qualitative evidence suggests the f orbitals play a role in the associated chemistry.[2] Moreover, recent direct evidence for f orbital-ligand interactions in early members of the actinide series has been observed by near-edge ligand X-ray absorption spectroscopy of $(C_5Me_5)_2AnCl_2$, An = Th, U.[3] Thus, while interactions with the 6d manifold may be stronger, modulations in the extent of 5f orbital involvement can affect the chemistry.

We report here that studies of the use of the metallocene amidinate coordination environments for actinides[4] have led to the synthesis of a rare example of a structurally characterizable trivalent thorium complex, $(C_5Me_5)_2[^iPrNC(Me)N^iPr]Th$. To date only three structurally characterized $Th^{3+}$ structures are known.[5−7] Since there is limited information on the electronic structure of this unusual oxidation state, hybrid density functional theory (DFT) calculations were carried out on this complex and its previously synthesized uranium analogue.[8] These results suggested that the analysis

*To whom correspondence should be addressed. E-mail: rlmartin@lanl.gov. (R.L.M.); wevans@uci.edu (W.J.E.)

(1) Bursten, B. E.; Strittmatter, R. J. *Angew. Chem., Int. Ed. Engl.* **1991**, *30*, 1069.
(2) See for example: (a) Pepper, M.; Bursten, B. E. *Chem. Rev.* **1991**, *91*, 719. (b) Li, J.; Bursten, B. E. *J. Am. Chem. Soc.* **1997**, *199*, 9021. (c) Diaconescu, P. L.; Arnold, P. L.; Baker, T. A.; Mindiola, D. J.; Cummins, C. C. *J. Am. Chem. Soc.* **2000**, *122*, 6108. (d) Meyer, K.; Mindiola, D. J.; Baker, T. A.; Davis, W. M.; Cummins, C. C. *Angew. Chem., Int. Ed.* **2000**, *39*, 3063. (e) Mazzanti, M.; Wietzke, R.; Pecaut, J.; Latour, J.-M.; Maldivi, P.; Remy, M. *Inorg. Chem.* **2002**, *41*, 2389. (f) Cantat, T.; Graves, C. R.; Jantunen, K. C.; Burns, C. J.; Scott, B. L.; Schelter, E. J.; Morris, D. E.; Hay, P. J.; Kiplinger, J. L. *J. Am. Chem. Soc.* **2008**, *130*, 17537.
(3) Kozimor, S. A.; Yang, P.; Batista, E. R.; Boland, K. S.; Burns, C. J.; Clark, D. L.; Conradson, S. D.; Martin, R. L.; Wilkerson, M. P.; Wolfsberg, L. E. *J. Am. Chem. Soc.* **2009**, *131*, 12125.
(4) Evans, W. J.; Walensky, J. R.; Ziller, J. W. *Organometallics* **2009**, *28*, 3350.
(5) Blake, P. C.; Lappert, M. F.; Atwood, J. L.; Zhang, H. *J. Chem. Soc., Chem. Commun.* **1986**, 1148.
(6) Parry, J. S.; Cloke, F. G. N.; Coles, S. J.; Hursthouse, M. B. *J. Am. Chem. Soc.* **1999**, *121*, 6867.
(7) Blake, P. C.; Edelstein, N. M.; Hitchcock, P. B.; Kot, W. K.; Lappert, M. F.; Shalimoff, G. V.; Tian, S. *J. Organomet. Chem.* **2001**, *636*, 124.
(8) Evans, W. J.; Walensky, J. R.; Ziller, J. W. *Chem.—Eur. J.* **2009**, *15*, 12204.


Published on Web 09/30/2010

should be extended to other trivalent actinides to gain a better understanding of the lesser studied actinides (Pa, Np, Pu, Am). Using the experimental anchor points with Th and U, we hoped to provide insight into the properties of the heavier actinides and stimulate synthetic interest in transuranic complexes of this type.

These efforts also provide molecular examples to compare with recent calculations on the tetravalent actinide series, $(C_5H_5)_4An$ (An = Th−Cm), [9] and screened hybrid DFT calculations on actinide dioxides that suggest that $PuO_2$ may actually have more covalent character than $UO_2$.[10] This is surprising, since the actinide contraction reflects a decrease in radial extension of the 5f orbitals and hence less overlap between metal and ligand orbitals. However, the orbital mixing depends not only on the orbital overlap but also on the orbital energy difference. In the case of the dioxides, the actinide 5f orbital remains well separated and higher in energy from ligand orbitals in the early members of the series, as verified from photoelectron spectroscopy, for example. However, the 5f orbital is also energetically stabilized with increasing $Z$ and so at some point becomes nearly degenerate with the O 2p orbitals. This finding in the solid actinide oxides warranted an examination in a molecular system with different types of ligands. The $(C_5Me_5)_2[^iPrNC(Me)N^iPr]An$ complexes provided the opportunity, and the results are reported here.

## Results

**Synthesis of $(C_5Me_5)_2[^iPrNC(Me)N^iPr]Th$, 1.** The reaction of the cationic complex, $\{(C_5Me_5)_2[^iPrNC(Me)N^iPr]Th\}\{BPh_3Me\}$,[8] made in situ from $BPh_3$ and $(C_5Me_5)_2[^iPrNC(Me)N^iPr]ThMe$, with $KC_8$ in tetrahydrofuran (THF) immediately produced a dark purple solution that persisted overnight, eq 1. Crystals suitable for X-ray diffraction were

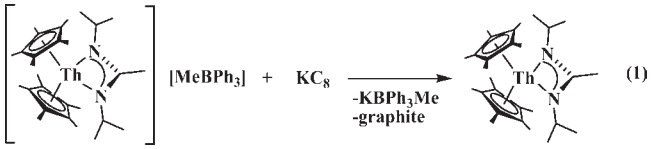


(1)

grown from a saturated $Et_2O$ solution at −35 °C that identified the purple product as the trivalent Th complex, $(C_5Me_5)_2[^iPrNC(Me)N^iPr]Th$, **1**, Figure 1 and Table 1. The isolation of **1** is remarkable because it was done in the presence of $N_2$, THF, and $Et_2O$. Previous attempts to make $Th^{3+}$ have led to reduced dinitrogen products,[11] deoxygenated[12,13] and ring-opened organic solvents,[14] as well as C−O, C−N, and C−H bond activation products.[15,16] Since the previously reported $U^{3+}$ analogue, $(C_5Me_5)_2[^iPrNC(Me)N^iPr]U$, displayed reduced $U^{3+}$ reactivity,[17] it is possible that the metallocene amidinate coordination environment is particularly effective in protecting $An^{3+}$ ions.

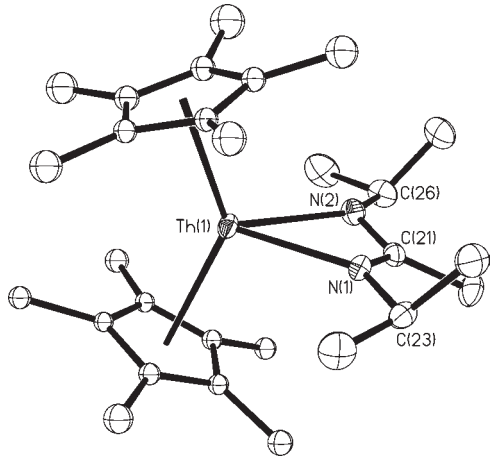


**Figure 1.** Thermal ellipsoid plot of $(C_5Me_5)_2[^iPrNC(Me)N^iPr]Th$, **1**, shown at the 50% probability level. Hydrogen atoms have been omitted for clarity.

**Table 1.** X-ray Data Collection Parameters for $(C_5Me_5)_2[^iPrNC(Me)N^iPr]Th$, **1**

| | |
|---|---|
| empirical formula | $C_{28}H_{47}N_2Th$ **1** |
| formula weight (g/mol) | 643.72 |
| temperature (K) | 98(2) |
| crystal system | monoclinic |
| space group | $P2_1/c$ |
| $a$ (Å) | 12.5758(15) |
| $b$ (Å) | 14.7777(18) |
| $c$ (Å) | 15.0404(18) |
| α (deg) | 90 |
| $\beta$ (deg) | 92.304(2) |
| $\gamma$ (deg) | 90 |
| volume (Å$^3$) | 2792.9(6) |
| $Z$ | 4 |
| $\mu_{calcd}$ (Mg/m$^3$) | 1.531 |
| (mm$^{-1}$) | 5.355 |
| R1 [$I > 2.0\sigma(I)$][a] | 0.0271 |
| wR2 (all data)[a] | 0.07 |

[a] $R1 = \sum||F_o| - |F_c||/\sum|F_o|$; $wR2 = [\sum w(F_o^2 - F_c^2)^2/\sum w(F_o^2)^2]^{1/2}$.

**Spectroscopy.** Because of the presence of one unpaired electron, complex **1** exhibited an EPR resonance with a $g$ value of 1.871 and no hyperfine. In comparison, a $g$ value of 1.916 was observed for $\{[\eta^8\text{-}C_8H_6(^tBuMe_2Si)_2\text{-}1,4]_2Th\}\{K(DME)_2\}$,[6] and a value of 1.910 was found for both $[C_5Me_3(SiMe_2{}^tBu)_2\text{-}1,3]_3Th$[7] and $[(C_5Me_3(SiMe_3)_2\text{-}1,3]_3Th$.[7,18] The purple complex displayed electronic transitions at 575 and 725 nm with extinction coefficients of about 2400. As described below, these were assigned to 6d to 5f transitions from the calculations.

**Structural Analysis.** Selected bond lengths and angles for **1** are compared with the three other examples in the literature in Table 2. The Th-(ring centroid) distances in **1** are rather similar to those in the tris(cyclopentadienyl) complexes, $[C_5Me_3(SiMe_3)_2]_3Th$ and $[C_5Me_3(SiMe_2{}^tBu)_2]_3Th$. Surprisingly, the 2.541 and 2.545 Å Th-($C_5Me_5$ ring centroid) lengths in **1** are shorter than the 2.584 and 2.598 Å in the tetravalent $(C_5Me_5)_2[^iPrNC(Me)N^iPr]ThMe$,[5] even though $An^{4+}$ ions usually have smaller radii

(9) Tassell, M. J.; Kaltsoyannis, N. *Dalton Trans.* **2010**, *39*, 6719.
(10) Prodan, I. D.; Scuseria, G. E.; Martin, R. L. *Phys. Rev. B* **2007**, *76*, 33101.
(11) Korobkov, I.; Gambarotta, S.; Yap, G. P. A. *Angew. Chem., Int. Ed.* **2003**, *42*, 4958.
(12) Korobkov, I.; Gambarotta, S.; Yap, G. P. A. *Angew. Chem., Int. Ed.* **2002**, *41*, 3433.
(13) Korobkov, I.; Arunachalampillai, A.; Gambarotta, S. *Organometallics* **2004**, *23*, 6248.
(14) Arunachalampillai, A.; Crewdson, P.; Korobkov, I.; Gambarotta, S. *Organometallics* **2006**, *25*, 3856.
(15) Arunachalampillai, A.; Gambarotta, S.; Korobkov, I. *Organometallics* **2005**, *24*, 1996.
(16) Korobkov, I.; Gambarotta, S.; Yap, G. P. A. *Angew. Chem., Int. Ed.* **2003**, *42*, 814.
(17) Evans, W. J.; Walensky, J. R.; Ziller, J. W. *Inorg. Chem.* **2010**, *49*, 1743.
(18) Kot, W. K.; Shalimoff, G. V.; Edelstein, N. M.; Edelman, M. A.; Lappert, M. F. *J. Am. Chem. Soc.* **1988**, *110*, 986.

**Table 2.** Comparison of Th-(Ring Centroid) Bond Distances (Å) and Angles (deg) in $(C_5Me_5)_2[^iPrNC(Me)N^iPr]Th$, **1**, with Other Structurally Characterized Trivalent Thorium Complexes

| bond distance/angle | **1** | $[C_5Me_3(SiMe_3)_2]_3Th$ | $[C_5Me_3(SiMe_2{}^tBu)_2]_3Th$ | $[\{COT(TBS)_2\}_2Th]K(DME)_2$ |
|---|---|---|---|---|
| Th−(ring centroid) | 2.541, 2.545 | 2.519, 2.526 | 2.532, 2.535 | 2.067, 2.094 |
| (ring centroid)−Th−(ring centroid) | 137.7 | 118.9, 120.0, 121.1 | 119.7, 119.8, 120.6 | 174.5 |

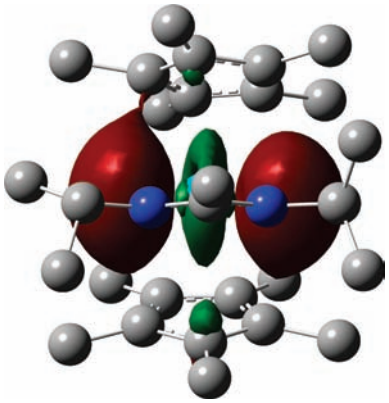

**Figure 2.** Singly Occupied Molecular Orbital (SOMO) in $(C_5Me_5)_2[^iPrNC(Me)N^iPr]Th$, **1**.

than $An^{3+}$ ions. The 2.476(3) and 2.482(3) Å Th−N bond distances in **1** are also shorter than the 2.509(2) and 2.515(2) Å analogues in $(C_5Me_5)_2[^iPrNC(Me)N^iPr]ThMe$.[5] The shorter bond distances in **1** can be attributed to the loss of the methyl group that allows the amidinate ligand to be closer to the metal center.

**Density Functional Theory Analysis.** Using the Heyd−Scuseria−Ernzerhof (HSE) functional,[19] the ground state of **1** is calculated to be a doublet with one unpaired electron localized in a $d_{z^2}$ orbital on thorium, Figure 2. The $5f^1$ state is estimated to be higher in energy by 0.91 eV according to time-dependent DFT (TD-DFT) results. Atomic charges using Mulliken analysis are notoriously difficult to interpret, but our experience is that orbital populations for more compact orbitals such as the 5f are less prone to these difficulties, nearly basis set independent, and usually conform to formal valence expectations. Given this caveat, we find the unpaired spin density (or spin polarization) on the Th site to be 0.94 electrons and largely resident in the d manifold (Table 4), consistent with a formal $Th^{3+}$, $6d^1$ configuration. There is some delocalization of spin onto the ligands, both to the amidinate and to the Cp moiety. The structural predictions (Table 3) are in reasonable agreement with experiment, although the calculated Th-amidinate distances are ~0.04 Å longer than the experimental values.

Table 3 presents calculated results for the remainder of the series. In all cases the high-spin $f^n$ (Hund's first rule) ground state was examined computationally. Beginning with Pa, the metal f orbitals become energetically more favorable and start to accommodate the unpaired spin. In Pa, the $f^2$ ground state was found to lie lowest; an initial guess of the form df collapsed to the $f^2$ configuration. For $U^{3+}$, where experimental structural data are available for comparison, the calculated U-amidinate bond distances are again overestimated by some 0.05 Å, typical of the errors found in hybrid DFT predictions for actinide complexes.[4,20]

## Discussion

The interplay between the actinide 6d and 5f orbitals is nicely demonstrated by the calculations of this series of $(C_5Me_5)_2[^iPrNC(Me)N^iPr]An$ complexes. In $Th^{3+}$, the unpaired spin is localized in the 6d orbital (Figure 2). The low-energy region of the experimental absorption spectrum (Supporting Information) shows two peaks at 725 nm and 575 nm. One expects these to involve transitions to the empty f-orbital manifold. The first seven excited states in our TD-DFT calculations are doublets, and natural transition orbital analysis[21] (Figure 4) show them to correspond to the expected seven d to f transitions. These range in energy from 0.9 eV (1300 nm) to 1.95 eV (636 nm). The lowest excited state at 0.9 eV carries little oscillator strength (0.0001). A pair of states in the region of 850−900 nm and another pair in the region of 635−690 nm carry most of the intensity and are presumably associated with the two experimental peaks. This would imply an error of some 0.3 eV in the computed excitation energies, not unreasonable given the problems when using TD-DFT with open-shell ground states.[22] In addition, we have neglected spin−orbit interactions in the calculations, which may introduce errors of this order of magnitude.

The next member of the series, $Pa^{3+}$, does not adopt a $d^1f^1$ configuration, but rather contains two unpaired electrons in 5f orbitals. This f orbital filling continues as Z increases. To illustrate the evolution of the 5f orbital energy across the series, we have plotted the molecular orbital eigenvalue spectrum for the series in Figure 3. For each eigenvalue, we present the orbital occupations—the molecular analogue of a partial density of states. As expected, there is systematic downward shift of the metal based 5f orbitals (red) as *Z* increases. The HOMO is indicated with an asterisk. For future reference, it is important to note that the metal 5f orbital energy becomes nearly degenerate with the ring based orbitals (black) in the vicinity of Np/Pu.

The associated spin densities are shown in Table 4. These show an unpaired spin count on the metal that is close to that expected from formal ionic charges. An important point to notice, however, is that the metal spin densities do not get closer to the formal predictions as *Z* increases, as one might expect if the bonding were entirely ionic in character. Rather, more unpaired spin density is shared/delocalized onto the ligands as *Z* increases.[9] In fact, at $Am^{3+}$, the unpaired spin density is 6.24, as opposed to the formal value of 6.0 expected from an $f^6$ ion. Since the remaining (minority) spin is found on the carbon atoms in the cyclopentadienyl ring, this implies that the metal is obtaining its additional spin from the $(C_5Me_5)^{1-}$ ligands and not very much from the amidinate ligand.

(19) Heyd, J.; Scuseria, G. E.; Emzerhof, M. *J. Chem. Phys.* **2003**, *118*, 8207.
(20) Graves, C. R.; Yang, P.; Kozimor, S. A.; Vaughn, A. E.; Clark, D. L.; Conradson, S. D.; Schelter, E. J.; Scott, B. L.; Thompson, J. D.; Hay, P. J.; Morris, D. E.; Kiplinger, J. L. *J. Am. Chem. Soc.* **2008**, *130*, 5272.
(21) Martin, R. L. *J. Chem. Phys.* **2003**, *118*, 4775.
(22) Dreuw, A.; Head-Gordon, M. *Chem. Rev.* **2005**, *105*, 4009.

**Table 3.** Calculated and Experimental Bond Distances and Angles

| | $(C_5Me_5)_2[^iPrNC(Me)N^iPr]An$ | | | | | | | |
|---|---|---|---|---|---|---|---|---|
| | An = Th | | An = Pa | An = U | | An = Np | An = Pu | An = Am |
| bond length (Å) and angle (deg) | calcd | expt | calcd | calcd | expt | calcd | calcd | calcd |
| An−N(1) | 2.494 | 2.476(3) | 2.511 | 2.464 | 2.435(3) | 2.457 | 2.454 | 2.441 |
| An−N(2) | 2.525 | 2.482(3) | 2.525 | 2.470 | 2.456(3) | 2.466 | 2.459 | 2.441 |
| An−C(21) | 2.961 | 2.898(4) | 2.958 | 2.905 | 2.869(4) | 2.896 | 2.895 | 2.872 |
| An−C($C_5Me_5$) average | 2.82 | 2.86(1) | 2.84 | 2.79 | 2.80(1) | 2.79 | 2.78 | 2.77 |
| N(1)−An−N(2) | 52.94 | 54.15(11) | 53.22 | 54.47 | 54.94(11) | 54.65 | 54.78 | 55.21 |

**Table 4.** Mulliken Atomic Spin Densities for $(C_5Me_5)_2[^iPrNC(Me)N^iPr]An$ Complexes

| | $(C_5Me_5)_2[^iPrNC(Me)N^iPr]An$ | | | | | |
|---|---|---|---|---|---|---|
| | An = Th | An = Pa | An = U | An = Np | An = Pu | An = Am |
| An | 0.942 | 2.038 | 3.079 | 4.149 | 5.168 | 6.241 |
| N(1) | −0.011 | −0.010 | −0.016 | −0.020 | −0.010 | −0.018 |
| N(2) | −0.014 | −0.010 | −0.019 | −0.022 | −0.012 | −0.019 |
| Amidinate C | 0.004 | 0.004 | 0.004 | 0.003 | −0.004 | 0.013 |
| Cp ring C | −0.011 | −0.043 | −0.054 | −0.099 | −0.157 | −0.223 |

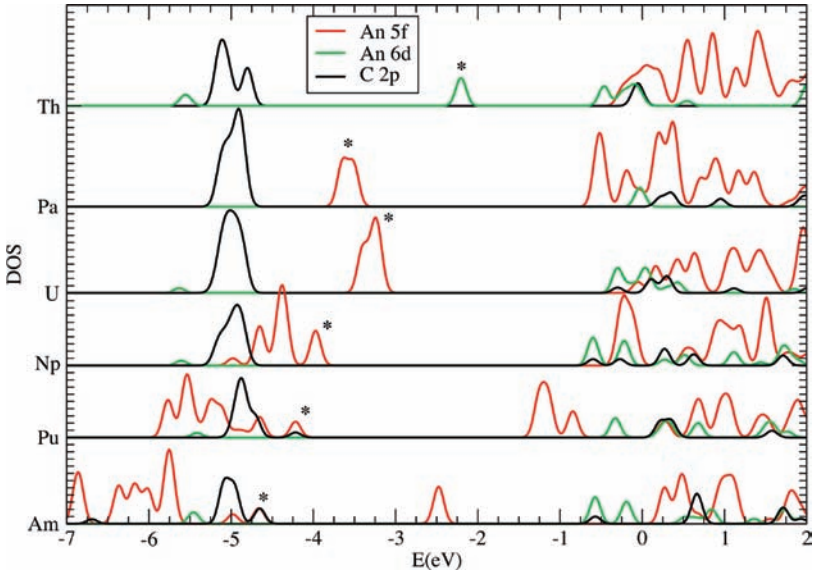


**Figure 3.** Density of States Plots for $(C_5Me_5)_2[^iPrNC(Me)N^iPr]An$, An = Th−Am. The percentage of atomic orbital character in each molecular orbital is plotted versus its B3LYP eigenvalue. The results are broadened with a Gaussian of width ~0.2 eV. The Fermi energies are indicated by an asterisk. In the Th complex the highest occupied molecular orbital (HOMO) is of 6d character; it quickly changes to f-like at Pa. Note that the states associated with the Cp ring (black) remain at the same energy (−5 eV) as Z increases, while the occupied f-like (red) states fall to lower energy as you progress along the series. Beginning with Np, there is some mixing evident between the two (as indicated by the small 5f component under the predominantly black C 2p peak). This is even more pronounced in the Pu complex; in Am these f-levels have largely dropped through the ring levels.

This trend in the spin densities as $Z$ increases initially seems counter-intuitive since the 5f orbitals are expected to contract with increasing $Z$ leading to less covalency. However, the calculations indicate significant orbital mixing and delocalization between the actinide 5f orbital and the cyclopentadienyl ring as $Z$ increases. The ring appears to become a more effective donor with increasing $Z$. Alternatively, the actinide is becoming a better acceptor, even though the formal ionic charge remains constant. The resulting spin polarization is being mediated by the metal 5f orbital. In view of the arguments of the introduction regarding orbital size variations with $Z$, how can this happen?

The origin of this effect is well-known, but sometimes forgotten in the context of actinide chemistry. Consideration of orbital overlap alone leads one to look for significant f orbital involvement in bonding in the early members of the series, before the actinide contraction reduces the orbital radius further. There is, however, another important contributor to efficient orbital mixing, and that is the relative energy between the 5f and appropriate ligand orbitals. In simple Hückel theory, if we denote these two orbitals as $\phi_f$ and $\phi_L$, then to the first order of perturbation theory, the resulting molecular orbital is given by

$$\psi = \phi_f + [\beta/(\varepsilon_f - \varepsilon_L)]\phi_L \quad (2)$$

where $\beta$ is directly proportional to the orbital overlap, and $\varepsilon$ denotes the orbital energy. The inadequate screening of the nucleus as the f shell fills leads not only to smaller orbitals, but also causes a dramatic reduction in the energy of the 5f orbitals. This is apparent in Figure 3. Note that the energy of the cyclopentadienyl $\pi$ orbital (black) is essentially unchanged with increasing $Z$, whereas the occupied actinide 5f orbitals (red) falls relentlessly as the series is traversed and crosses into

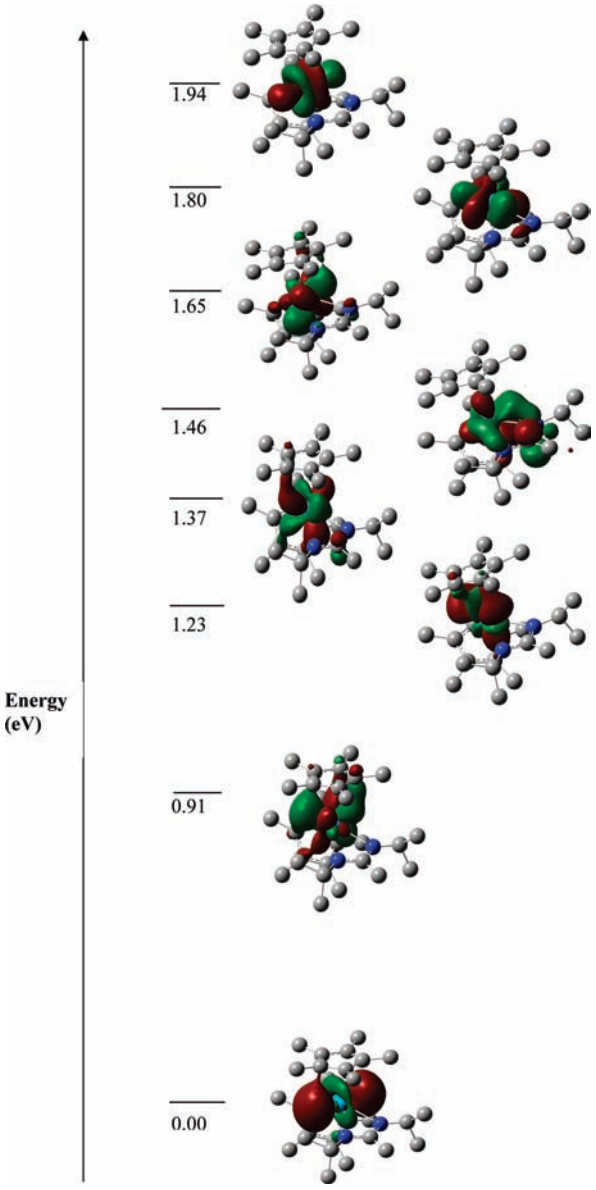


**Figure 4.** Natural Transition Orbitals for $(C_5Me_5)_2[^iPrNC(Me)N^iPr]Th$, **1**.

the region of the ligand $\pi$ near Np/Pu. Our calculations suggest that the decrease in the denominator of eq 2 is sufficient to overcome to some degree the decrease in the numerator, with the result that there is more significant ligand−metal interaction in the later members of this series.

This is reminiscent of the situation found in recent calculations on a series of crystalline actinide dioxides.[10] Deviations from formal ionic expectations were observed as $Z$ increased, reflecting increased covalency. While hybrid DFT yielded a very ionic picture for $UO_2$, significant An 5f /O 2p orbital mixing was observed in $PuO_2$, leading to substantial dispersion in the valence bands. In fact, the calculations found so much O 2p to metal charge transfer in $CmO_2$, that it is probably best described as intermediate valence, in the sense that the spin density reflects a metal valence between 3+ and 4+. Note that a formal metal valence of 3+ in an $AnO_2$ compound implies oxygen valencies smaller than 2−. This is not a sustainable situation. The valence requirements of $O^{2-}$ and $An^{3+}$ can be met with the stoichiometry $An_2O_3$. The sesquioxide does indeed become the more stable phase as $Z$ increases. In fact, only the sesquioxide has been synthesized in the later members of the series.

The important role of the energy denominator is well-known, but sometimes forgotten in these materials. Early indications of significant interaction occurring in later members of the series were seen in DVXα calculations on $AnO_6$ clusters by Gubanov, Rosen, and Ellis,[23] and in $(C_5H_5)_4An$ compounds by Kaltsoyannis and Bursten.[24] The general issue of covalency in these materials was recognized early by Pyykko.[25] Here we simply wish to point out that the influence of the orbital energy difference on bonding in the actinide series is often overlooked, and may have surprising consequences. We emphasize that our point is principally a qualitative one; our omission of spin−orbit coupling and errors in our functionals may alter the details of the energy−level crossover, but will not change our major conclusion. An issue still to be determined is whether this enhanced mixing implies "covalency" in the sense of increased metal−Cp bond energies. This issue is currently being investigated.

## Conclusion

We have reported the rare synthesis and structural characterization of a trivalent thorium complex and the first with a non-hydrocarbon ligand. A DFT analysis of the structurally characterized $Th^{3+}$ and $U^{3+}$ complexes was extended to trivalent metallocene amidinate complexes of the actinides from Th−Am. The calculations suggest increased orbital mixing and spin delocalization as one progresses from the left to the right across the actinide series.

## Experimental Section

***Caution!*** *Thorium (primarily $^{232}Th$) is a weak alpha-emitter with a half-life of $1.41 \times 10^{10}$ years and should only be used with the appropriate safety and equipment.*

The syntheses and manipulations described below were conducted with rigorous exclusion of air and water using Schlenk, vacuum line, and glovebox techniques. Solvents were sparged with UHP argon, dried by passage through columns containing Q-5 and molecular sieves, and delivered directly to the glovebox through stainless steel tubing. Benzene-$d_6$ (Cambridge Isotope Laboratories) was dried over NaK alloy and benzophenone, degassed by three freeze−pump−thaw cycles, and vacuum transferred before use. $BPh_3$ (Aldrich) was sublimed prior to use. $(C_5Me_5)_2[^iPrNC(Me)N^iPr]ThMe$ was made according to the literature.[4] Infrared spectra were recorded as KBr pellets on a Perkin-Elmer Spectrum One FT-IR spectrometer. Elemental analyses were performed with a Perkin-Elmer 2400 CHN elemental analyzer. UV/vis absorbance spectra (250−800 $nm^{-1}$) were recorded on a Perkin-Elmer Lambda 800 double-beam spectrophotometer equipped with a PMT detector. EPR spectra were recorded with a Bruker EMX spectrometer equipped with a standard $TE_{102}$ (ER 4102ST) resonator (Bruker).

**$(C_5Me_5)_2[^iPrNC(Me)N^iPr]Th$, 1.** In a nitrogen atmosphere glovebox, freshly sublimed $BPh_3$ (163 mg, 0.673 mmol) was added to a stirred solution of $(C_5Me_5)_2[^iPrNC(Me)N^iPr]ThMe$ (440 mg, 0.668 mmol) in THF (10 mL). The color immediately turned from colorless to bright yellow. After 5 min, $KC_8$ (40 mg, 1.0 mmol) was added, and the color immediately turned dark

(23) Gubanov, V. A.; Rosen, A.; Ellis, D. E. *J. Phys. Chem. Solids* **1979**, *40*, 17.
(24) Kaltsoyannis, N.; Bursten, B. E. *J. Organomet. Chem.* **1997**, *528*, 19.
(25) Pyykko, P.; Li, J.; Runeberg, N. *J. Phys. Chem.* **1994**, *98*, 480.

purple. After 12 h, insoluble material was removed by centrifugation, and the solvent removed under vacuum to yield **1** as a dark purple powder (370 mg, 86%). Crystals suitable for X-ray diffraction were grown from a saturated $Et_2O$ solution at −35 °C. IR (KBr): 2970s, 2858 m, 1639 m, 1530 m, 1419s, 1377s, 1328s, 1301s, 1190s, 1183 m, 1038 m, 932s, 803s, 759s $cm^{-1}$. Anal. Calcd for $C_{28}H_{47}N_2Th$: C, 52.24; H, 7.36; N, 4.35. Found: C, 52.07; H, 7.49; N, 4.26.

**Computational Details.** Electronic structure calculations were conducted using the hybrid HSE1PBE[19] functional in the Gaussian09 code.[26] The Stuttgart 97 relativistic effective core potential (RECP) and associated basis sets were used for the metal atoms, except that the most diffuse s, p, d, and f functions were removed leaving a 7s/6p/5d/3f set. The 6-31G* basis set was used for C, H, and N atoms. These basis sets have been used extensively for organometallic complexes and have been shown to give good agreement with experimental data.[4,20]

(26) Frisch, M. J. et al. *Gaussian 09*, Revision A.02; Gaussian, Inc.: Wallingford, CT, 2009.

**Acknowledgment.** We thank the Chemical Sciences, Geosciences, and Biosciences Division, and the Heavy Element Chemistry program of the Office of Basic Energy Sciences of the Department of Energy for support of this research. We also thank Dr. Michael K. Takase for assistance with X-ray crystallography and Nathan A. Siladke for assistance with the UV−visible spectroscopy. The Glenn T. Seaborg Institute at LANL is gratefully acknowledged for funding (J.R.W.). This work was carried out under the auspices of the National Nuclear Security Administration of the U.S. Department of Energy at Los Alamos National Laboratory under Contract DE-AC5206NA25396.

**Supporting Information Available:** Crystallographic data in CIF format and further details in the form of Tables A−L and Figure A. This material is available free of charge via the Internet at http://pubs.acs.org.